

Biophysical Journal, Volume 98

Supporting Material

Antimicrobial Protegrin-1 (PG-1) Forms Ion Channels: MD Simulation, AFM, and Electrical Conductance Studies

Ricardo Capone, Mirela Mustata, Hyunbum Jang, Fernando Teran Arce, Ruth Nussinov, and Ratnesh Lal

Supporting Information

Antimicrobial Protegrin-1 Forms Ion Channels: Molecular Dynamic Simulation, Atomic Force Microscopy, and Electrical Conductance Studies

Ricardo Capone^{†,Δ}, Mirela Mustata^{†,Δ}, Hyunbum Jang^{‡,Δ}, Fernando Teran Arce[†], Ruth Nussinov^{‡,Δ,§,*} and Ratnesh Lal^{†,Δ,*}

[†]Center for Nanomedicine and Department of Medicine, University of Chicago, Chicago, Illinois; [‡]Center for Cancer Research Nanobiology Program, NCI-Frederick, SAIC-Frederick, Inc., Frederick, Maryland; and [§]Sackler Inst. of Molecular Medicine, Department of Human Genetics and Molecular Medicine, Sackler School of Medicine, Tel Aviv University, Tel Aviv, Israel

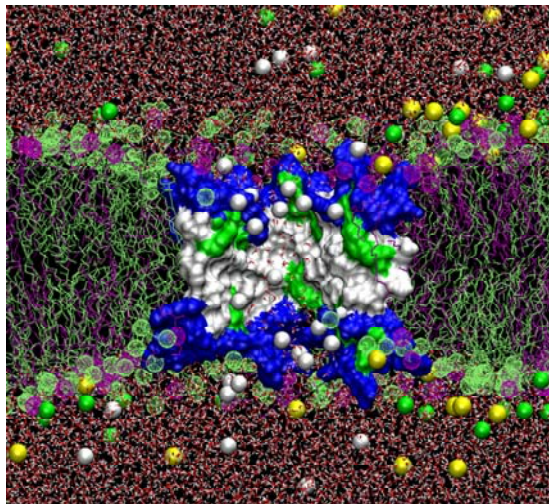
^Δ These authors contributed equally. ^ΔR.N. and R.L. laboratories contributed equally to the work

*Correspondence to: rlal@uchicago.edu
ruthnu@helix.nih.gov

R. Capone, F.T. Arce and R. Lal present address is: Bioengineering and Mechanical and Aerospace Engineering, University of California San Diego, La Jolla, CA 92093, U.S.A

Running title: Antimicrobial PG-1 forms ion channel

A Antiparallel β -sheet PG-1 channel



B Parallel β -sheet PG-1 channel

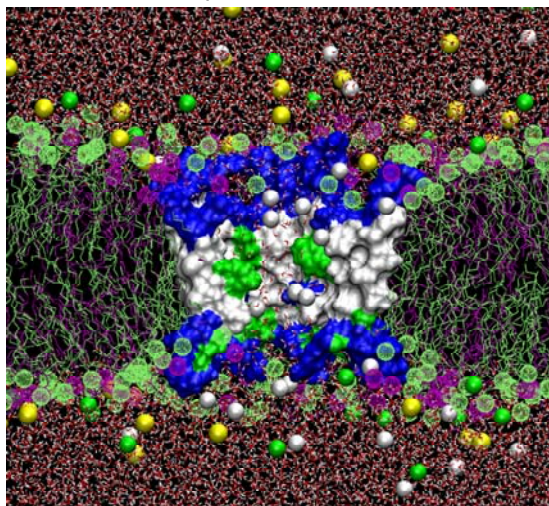


FIGURE S1 Snapshots at 30 ns for the (A) antiparallel and (B) parallel β -sheet channels of PG-1 in the DOPS/POPE: (1:2) bilayer. In the surface representation for the channels, the front part of the channels in the lateral view has been removed to allow a view of the pore. In the channel structures, hydrophobic residues are shown in white, polar and Gly residues are shown in green, and positively charged residues are shown in blue. The lipids tails are shown as thread in lime color for POPE and in purple for DOPS. Phosphate atoms in the lipid head group are shown as meshed sphere with the same colors as in the lipid tails. Water molecules are shown in tiny red (oxygen) and white sticks (hydrogen). Mg²⁺ is shown in green bead, Na⁺ is shown in yellow bead, and Cl⁻ is shown in white bead.

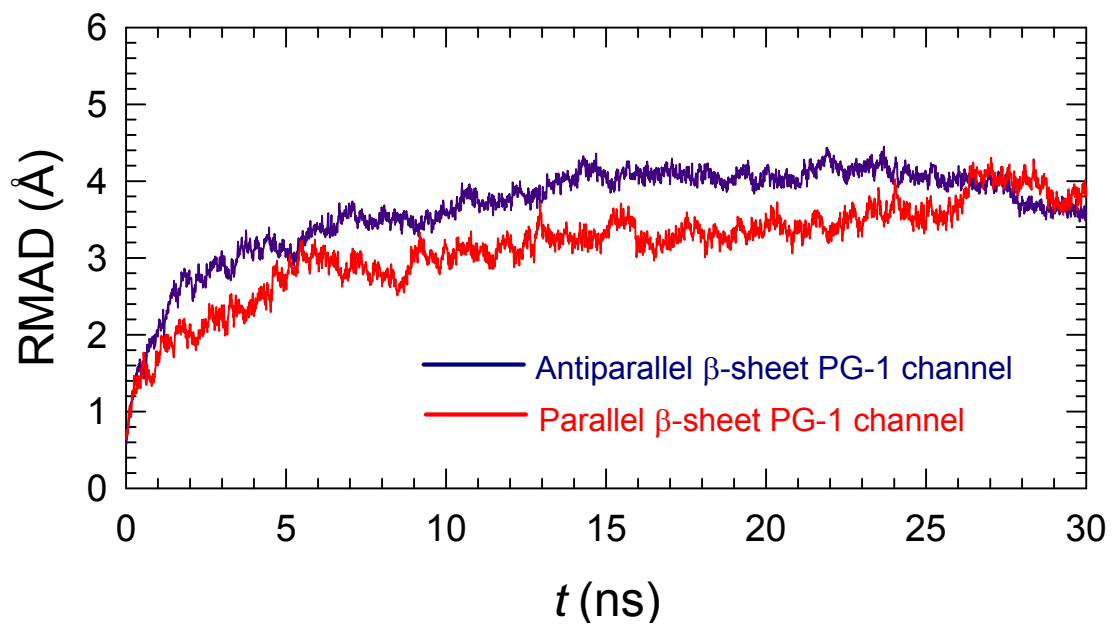


FIGURE S2 Time series of the root-mean-squared-deviation (RMSD) from the starting point for backbone atoms in the antiparallel (blue line) and parallel (red line) β -sheet PG-1 channels.

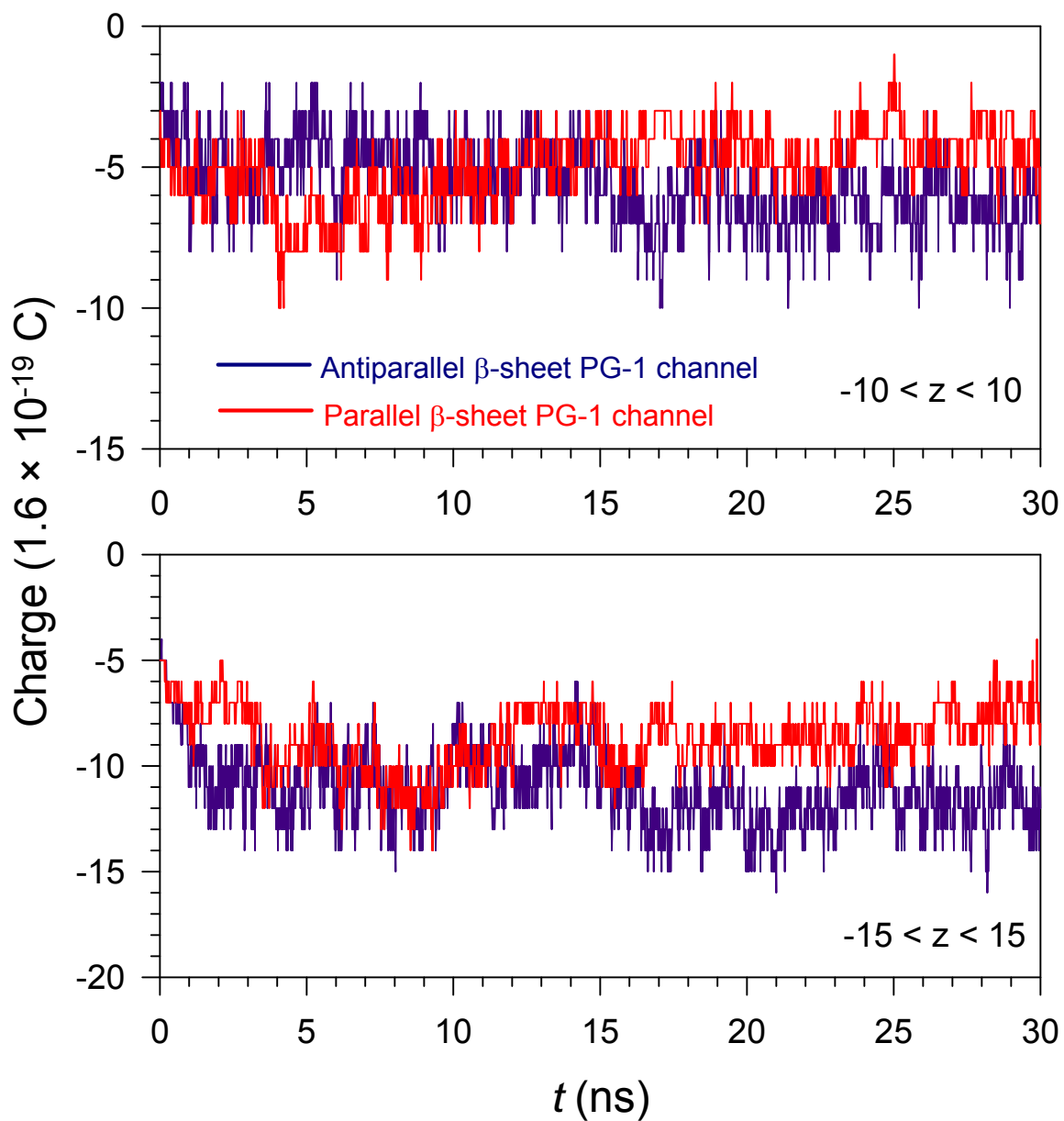


FIGURE S3 Time series of the charged state induced by ions (Mg^{2+} , Na^+ , and Cl^-) in the pore of the antiparallel (blue lines) and parallel (red lines) β -sheet PG-1 channels. The number of charges are counted in the pore with cutoffs, $-10 \text{ nm} < z < 10 \text{ nm}$ (upper panel) and $-15 \text{ nm} < z < 15 \text{ nm}$ (lower panel), from the bilayer center along the pore axis.

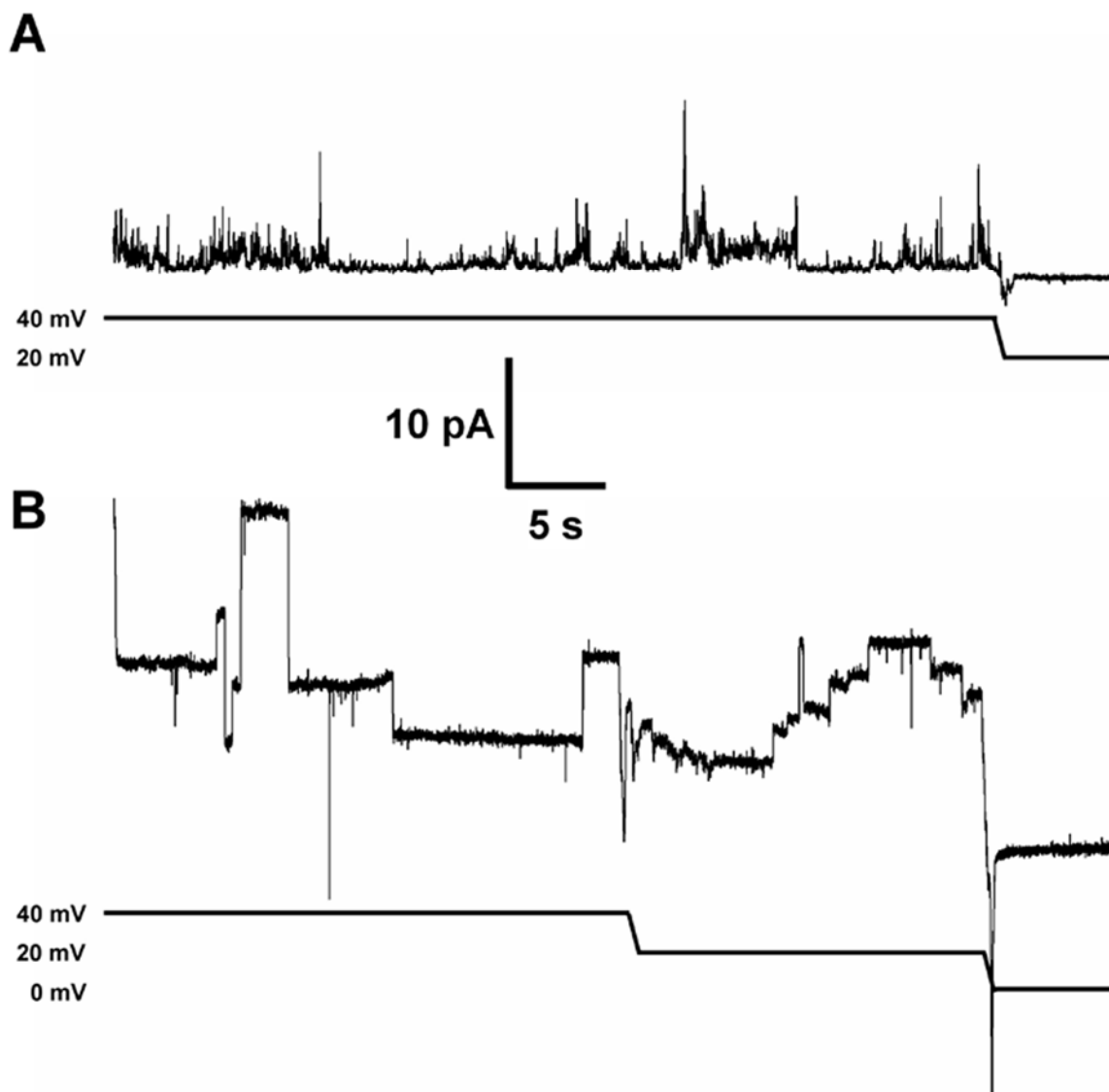


FIGURE S4 Comparative behavior of PG-1 in PS/PE (1:1) bilayers obtained by either the folded (A) or painted methods (B). Similar PG-1 concentrations tend to elicit a spikier and short-lived channel behavior in folded bilayers when compared to painted bilayers. Events seem to have comparable current amplitudes, but given the multiple conductances present in these lipid compositions, it is difficult to conclusively state that. The traces are recorded at various voltages as shown below each trace. The electrolyte used was 100 mM KCl, 10 mM HEPES and 1 mM $MgCl_2$. PG-1 was added into one side of the bilayer chamber.

SUPPORTING MATERIALS AND METHODS

Chemicals

n-hexane, *n*-heptane, KCl, ZnCl₂ and Hepes were from Sigma-Aldrich (St Louis MO). Lipids 1-palmitoyl-2-oleoyl-*sn*-glycero-3-phosphoethanolamine (POPE), 1,2-diphytanoyl-*sn*-glycero-3-phosphocholine (DiPhyPC), 1,2-dioleoyl-*sn*-glycero-3-phospho-L-serine (DOPS), 1,2-dioleoyl-*sn*-glycero-3-phosphoethanolamine (DOPE), and 1,2-dioleoyl-*sn*-glycero-3-phosphatidylcholine (DOPC) were from Avanti Polar Lipids (Birmingham, AL). The PG-1 peptide, synthesized in Dr. Carl Saxinger lab at the NCI-Frederick, was dissolved in 0.01% acetic acid to 1 mg/mL concentration and aliquoted. Aliquots were thawed only once.

Molecular Dynamics (MD) Simulations

The PG-1 channels were made with ten identical β -hairpins of PG-1, initially arranged to form a perfect annular shape of a single layer β -sheet. We used the prerelaxed β -hairpin structure obtained from preliminary simulations of the solution NMR structure of the PG-1 monomer (1) in the lipid environment, as described in previous simulations (2). Depending on the β -hairpin arrangement, the PG-1 channel has two potential β -sheet motifs; antiparallel (turn-next-to-tail) and parallel (turn-next-to-turn) β -sheets in a multimeric NCCN packing mode (3). The channel is minimized with a rigid body motion for the peptides to enhance the formation of intermolecular backbone H-bonds between the β -strands. The minimized channel is next embedded in the lipid bilayer containing DOPS/POPE (mole ratio 1:2). For the bilayer topology, the intrinsic barrel-stave membrane pore was initially prepared for the β -sheet channels (4).

Next, we construct a unit cell containing a single channel, lipids, salts, and waters; overall using almost 152,000 atoms. Because the simulation method here closely follows the protocol previously described for the PG-1 monomer (5), dimer (6), octamer (2), A β channels (7,8), and K3 channels (9) simulations, in this study we only describe briefly key parameters used for the decameric PG-1 channel simulations. For the lipid bilayer, 420 lipids (140 DOPS and 280 POPE lipids) constitute the lateral cell. TIP3P waters were added and relaxed through a series of minimization and dynamics. The system contains MgCl₂ and NaCl at the same concentration of 50 mM to satisfy a total cation concentration of approximately 100 mM. The CHARMM program (10) was used to construct the set of starting points and to relax the systems to a production-ready stage. For production runs to 30 ns, the NAMD code (11) on a Biowulf cluster at the NIH was used for the starting point. Averages were taken after 10 ns discarding initial transient.

In addition to the decameric PG-1 channel simulations, we also performed the simulations for the decameric PG-1 fibrils on the surface of the same anionic lipid bilayer. The decameric PG-1 fibril was initially constructed as a linear shape. Two different β -sheet motifs, antiparallel (turn-next-to-tail) and parallel (turn-next-to-turn) β -sheets in a multimeric NCCN packing mode (3), were also used in the fibril constructions. For the lipid bilayer, 480 lipids (160 DOPS and 320 POPE lipids) constitute the lateral cell with almost 160,000 atoms. A series of minimization and dynamics for the PG-1 fibril/lipid system were performed with the same simulations parameters used for the PG-1 channel simulations.

Sample Preparation for AFM Imaging

For AFM imaging of peptides on mica, a 1mg/mL aliquot was sonicated in the ice-water bath for 20-30 min. PG-1 was diluted to the final concentration of 200-300 $\mu\text{g/mL}$ by adding PBS. A 50 μL droplet of this solution was then deposited on mica and imaged after a few minutes.

For AFM imaging of the peptides reconstituted in lipid bilayers, the samples were prepared following the protocols described by previously published protocols (12,13). The lipid mixture of 1:1 (w/w) DOPS/POPE dissolved in chloroform was vacuum-dried. The peptide solution, diluted in PBS, was used to hydrate the lipid cake to concentrations of 300-500 $\mu\text{g/mL}$. This was followed by 15 min vortexing and 20-30 min sonication in an ice-water bath kept at ~ 4 $^{\circ}\text{C}$. A 50 μL droplet of a solution of peptides reconstituted in liposomes was allowed to adsorb for 5-15 min on freshly cleaved mica to create a supported lipid bilayer with pre-incorporated peptides. The sample was rinsed 3 times with PBS to eliminate all unincorporated peptides as well as liposomes that were not ruptured.

AFM Imaging and Image Analysis

AFM images were acquired using a 5.30 Nanoscope controller with an Extender electronics module (Veeco, Santa Barbara, CA). Oxide-sharpened silicon nitride cantilevers with nominal spring constants (k_n) of 0.12 N/m (Veeco, Santa Barbara, CA) were used to image PG-1 peptides on mica. TR400PB Olympus cantilevers (Asylum Research, Santa Barbara, CA) with $k_n=0.02$ N/m were used for imaging PG-1 reconstituted in lipid bilayers. Images were acquired in tapping mode at scan frequencies of 0.5-1 Hz and drive amplitudes below 100 mV. The cantilever oscillation frequency was 5-10 Hz. All scans were performed in PBS at room temperature using a fluid cell from Veeco. Image analysis was performed using the Veeco software (13). Some AFM images were low-pass filtered to remove noise. Sizes of the reconstituted channels in the membrane were obtained from the height images using cross-sectional analysis. Channel diameters were measured at two-thirds full height with respect to the lipid bilayer surface.

Formation of Planar Lipid Bilayers

We generated vertical planar lipid bilayers (PLBs) by either the painting (14) or the folding methods (15). As electrolyte we used in both methods 100 mM KCl, 10 mM HEPES pH 7.4 and 1 mM MgCl_2 . For painted membranes we applied lipid mixtures of DOPS/POPE 1:1 (w/w, 20 mg/ml in heptane) over a pore. We used bilayer cups made of Delrin with a pore diameter of ~ 250 μm in a Delrin septum (Warner Instruments, Delrin perfusion cup, volume 1 ml) pretreated with the same lipid mixture dissolved in hexane (9,16). Prior to painting the membrane we verified that the electrode asymmetry was always less than 1 mV. Upon membrane formation we screened for membranes that were stable and had conductances of less than 10 pS up to voltages of ± 100 mV for a period of at least 10 min with capacitances higher than 100 pF (typically ~ 150 pF). When the above three criteria were fulfilled, we added 2 to 40 μL of PG-1 dissolved in 0.01% acetic acid leading to final concentrations in the range of 0.25 to 10 μM to the *cis* compartment (hotwire) and stirred for 1-2 min. For the folded membranes we used a Teflon film (Eastern Scientific Inc, pore diameter ~ 0.1 mm) pretreated on each side with 2 μL of 5% hexadecane in pentane and allowed solvent evaporation. This film was then mounted using

vacuum grease (Dow Corning, High vacuum grease) to a custom-made Teflon chamber separating two buffer compartments each with a volume capacity of 3 mL. After addition of 1 mL of electrolyte to each compartment, lipids were spread from a solution in pentane onto the surface of the electrolyte solutions (specifically, we added 4–6 μL from 25 mg/mL solutions pure DiPhyPC (17), DOPC or 1:1 (w/w) mixtures of DOPS/DOPE, DOPC/DOPE (16) on top of the recording buffer in the bilayer chamber). Two additional milliliters of electrolyte solution were added to each side of the chamber to raise the liquid levels above the aperture. We formed the bilayers from apposition of two monolayers of lipids (14,15) until a bilayer was obtained that had a minimum capacitance of 70-90 pF and until the resulting membrane was stable (i.e., no significant current fluctuations above the baseline noise level) in the range of ± 100 mV applied potential for 10 minutes. When these criteria were satisfied, we added PG-1 as indicated above. We found that often in our bilayer-chamber the use of DOPC formed unstable bilayers prior to addition of PG-1; we hence focused with DiPhyPC to form PC bilayers.

Bilayer System and Data Analysis

We performed all recordings using an EPC-7 amplifier on “voltage clamp mode” (set at a gain of 10 mV pA^{-1} and a filter cutoff frequency of 3 kHz) using Ag/AgCl electrodes. Data acquisition and storage was carried out using custom software (18). Sampling frequency was set at 15 kHz for all bilayer experiments. Analysis of the single channel current traces was done by computing histograms of the current-time traces with ClampFit 9.2 software from Axon Instruments. For representation in figures, we filtered the current traces with a digital Gaussian low-pass filter with a cutoff frequency of 100 Hz.

SUPPORTING REFERENCES

1. Fahrner, R. L., T. Dieckmann, S. S. Harwig, R. I. Lehrer, D. Eisenberg, and J. Feigon. 1996. Solution structure of protegrin-1, a broad-spectrum antimicrobial peptide from porcine leukocytes. *Chem. Biol.* 3:543-550.
2. Jang, H., B. Ma, R. Lal, and R. Nussinov. 2008. Models of toxic beta-sheet channels of protegrin-1 suggest a common subunit organization motif shared with toxic Alzheimer beta-amyloid ion channels. *Biophys. J.* 95:4631-4642.
3. Tang, M., A. J. Waring, and M. Hong. 2005. Intermolecular Packing and Alignment in an Ordered β -Hairpin Antimicrobial Peptide Aggregate from 2D Solid-State NMR. *J. Am. Chem. Soc.* 127:13919-13927.
4. Jang, H., B. Ma, R. Lal, and R. Nussinov. 2008. Models of toxic beta-sheet channels of protegrin-1 suggest a common subunit organization motif shared with toxic Alzheimer beta-amyloid ion channels. *Biophys. J.* 95:4631-4642.
5. Jang, H., B. Ma, T. B. Woolf, and R. Nussinov. 2006. Interaction of protegrin-1 with lipid bilayers: membrane thinning effect. *Biophys. J.* 91:2848-2859.
6. Jang, H., B. Ma, and R. Nussinov. 2007. Conformational study of the protegrin-1 (PG-1) dimer interaction with lipid bilayers and its effect. *BMC Struct. Biol.* 7:21.
7. Jang, H., J. Zheng, R. Lal, and R. Nussinov. 2008. New structures help the modeling of toxic amyloids ion channels. *Trends Biochem. Sci.* 33:91-100.
8. Jang, H., J. Zheng, and R. Nussinov. 2007. Models of beta-amyloid ion channels in the membrane suggest that channel formation in the bilayer is a dynamic process. *Biophys. J.* 93:1938-1949.
9. Mustata, M., R. Capone, H. Jang, F. T. Arce, S. Ramachandran, R. Lal, and R. Nussinov. 2009. K3 fragment of amyloidogenic beta(2)-microglobulin forms ion channels: implication for dialysis related amyloidosis. *J. Am. Chem. Soc.* 131:14938-14945.
10. Brooks, B. R., R. E. Bruccoleri, B. D. Olafson, D. J. States, S. Swaminathan, and M. Karplus. 1983. Charmm - a Program for Macromolecular Energy, Minimization, and Dynamics Calculations. *J. Comp. Chem.* 4:187-217.
11. Phillips, J. C., R. Braun, W. Wang, J. Gumbart, E. Tajkhorshid, E. Villa, C. Chipot, R. D. Skeel, L. Kale, and K. Schulten. 2005. Scalable Molecular Dynamics with NAMD. *J. Comp. Chem.* 26:1781-1802.
12. Lin, H., R. Bhatia, and R. Lal. 2001. Amyloid beta protein forms ion channels: implications for Alzheimer's disease pathophysiology. *Faseb J.* 15:2433-2444.

13. Quist, A., I. Doudevski, H. Lin, R. Azimova, D. Ng, B. Frangione, B. Kagan, J. Ghiso, and R. Lal. 2005. Amyloid ion channels: a common structural link for protein-misfolding disease. *Proc. Natl. Acad. Sci. USA* 102:10427-10432.
14. Mueller, P., D. O. Rudin, H. T. Tien, and W. C. Wescott. 1962. Reconstitution of cell membrane structure in vitro and its transformation into an excitable system. *Nature* 194:979-980.
15. Montal, M. and P. Mueller. 1972. Formation of bimolecular membranes from lipid monolayers and a study of their electrical properties. *Proc. Natl. Acad. Sci. USA* 69:3561-3566.
16. Capone, R., F. G. Quiroz, P. Prangkio, I. Saluja, A. M. Sauer, M. R. Bautista, R. S. Turner, J. Yang, and M. Mayer. 2009. Amyloid-beta-induced ion flux in artificial lipid bilayers and neuronal cells: resolving a controversy. *Neurotox. Res.* 16:1-13.
17. Capone, R., S. Blake, M. R. Restrepo, J. Yang, and M. Mayer. 2007. Designing nanosensors based on charged derivatives of gramicidin A. *J. Am. Chem. Soc.* 129:9737-9745.
18. Macrae, M. X., S. Blake, X. Jiang, R. Capone, D. J. Estes, M. Mayer, and J. Yang. 2009. A Semi-Synthetic Ion Channel Platform for Detection of Phosphatase and Protease Activity. *ACS Nano* 3:3567-3580.